

Concentration quenching in $\text{Nd}_x\text{Y}_{1-x}\text{P}_5\text{O}_{14}$ crystals

John M. Flaherty* and Richard C. Powell

Department of Physics, Oklahoma State University, Stillwater, Oklahoma 74074

(Received 22 May 1978)

An extensive investigation of the spectroscopic properties of $\text{Nd}_x\text{Y}_{1-x}\text{P}_5\text{O}_{14}$ is reported. Time-resolved site-selection spectroscopy and photoacoustic spectroscopy techniques were used as well as standard optical spectroscopy measurements which were made as a function of Nd concentration, temperature, excitation wavelength, and laser power. Results show that Nd ions occupy a variety of slightly perturbed sites. No significant energy transfer appears to be taking place between ions in these inequivalent sites. Additional experimental data presented here suggest a new quenching model for neodymium pentaphosphate crystals based on spatial but nonspectral energy migration to surface quenching sites.

I. INTRODUCTION

The development of the technology of fiber optics has resulted in a requirement for miniature optically pumped lasers with low threshold and high gain.¹ Stoichiometric laser materials such as neodymium pentaphosphate ($\text{NdP}_5\text{O}_{14}$) meet these requirements.²⁻⁴ Despite the significant amount of work that has been done recently, there are still some aspects of the luminescence properties of concentrated Nd materials that are not well understood. Complete characterization of the optical properties of this class of materials is important not only for technological design considerations but also for obtaining a basic understanding of the physical interaction mechanisms involved.

The most important property of stoichiometric laser materials is that they exhibit unusually weak concentration quenching. This allows the concentration of neodymium ions in $\text{NdP}_5\text{O}_{14}$ to be very high without significant degradation of the fluorescence and lasing properties of the material. The characteristics of the concentration quenching in stoichiometric laser materials are different from those in other well-characterized materials such as $\text{Y}_3\text{Al}_5\text{O}_{12}:\text{Nd}^{3+}$, and the physical mechanism for the quenching process is not understood at this time. Developing a model to explain concentration quenching in $\text{NdP}_5\text{O}_{14}$ is an important problem in understanding this class of materials.

To date, three basic mechanisms have been proposed to explain the concentration-quenching characteristics of stoichiometric laser materials. All have been proven unsatisfactory. The first mechanism postulated was cross relaxation between pairs of Nd ions in the bulk of the crystal, which predicted a quadratic concentration dependence for the quenching rate.⁵⁻⁸ This prediction is inconsistent with experimental results.¹⁻⁹ A second suggestion for a quenching

mechanism involved crystal-field overlap mixing effects between Nd^{3+} ions,¹⁰ but this has been proved wrong by the observation that the oscillator strengths of the Nd^{3+} transitions are independent of concentration.¹¹ Finally, energy migration to ions in randomly distributed sites throughout the bulk of the crystal acting as "sinks" where the energy is dissipated radiationlessly has been proposed.^{6,7,9,12} Unfortunately, this model requires the unrealistic assumption that the concentration of ions in quenching sites is the same for all samples independent of total Nd concentration.⁹ We recently reported preliminary results indicating that spectral energy transfer between Nd^{3+} ions in slightly different types of sites is not taking place in $\text{NdP}_5\text{O}_{14}$ as it does in materials such as $\text{Y}_3\text{Al}_5\text{O}_{12}:\text{Nd}^{3+}$, even at low concentrations.¹³

In this paper we report the results of an investigation of the mixed-crystal system of $\text{Nd}_x\text{Y}_{1-x}\text{P}_5\text{O}_{14}$ where we have utilized some new spectroscopic techniques in an attempt to better understand the concentration-quenching mechanism in these materials. Laser time-resolved site-selection spectroscopy was used to investigate energy transfer, and the results show that migration among Nd^{3+} ions in nonequivalent sites does not take place. Photoacoustic spectroscopy (PAS) measurements were made to characterize radiationless relaxation processes among the excited states of Nd^{3+} in these materials. The results are not consistent with those expected for PAS signals originating mainly from those phonons due to relaxation processes from higher absorption levels to the metastable level. A model based on surface quenching of the excitation is proposed which can explain the observed PAS results, and is consistent with all the other spectroscopic observations obtained on this material. The possible mechanisms for the quenching process and the effects of radiative reabsorption are also discussed.

II. SAMPLES AND EXPERIMENTAL EQUIPMENT

The $\text{NdP}_5\text{O}_{14}$ crystal was grown from solution at Philips Laboratory while the mixed crystals were grown at the Army Electronics Command Laboratories. Six samples of $\text{Nd}_x\text{Y}_{1-x}\text{P}_5\text{O}_{14}$ ranging from $x = 1.00$ to $x = 0.10$ were investigated. These consisted of small crystallites varying in size from about 2.0 mm on a side to about 0.50 mm.

For optical-spectroscopy measurements, the samples were mounted in a cryogenic refrigerator to control the temperature. For PAS the samples were mounted in an acoustical cavity and the signal detected by a 1-in. electret microphone. The excitation source for obtaining PAS and fluorescence excitation spectra was a 1000-W tungsten-halogen lamp passed through a $\frac{1}{4}$ -m monochromator. For measuring fluorescence lifetimes and obtaining time-resolved spectroscopy data, the excitation source was a nitrogen-laser-pumped tunable dye laser with rhodamine 6-G dye. This provided a pulse of about 10 nsec in duration and less than 0.5 \AA in half-width. Sample emission was analyzed by a 1-m monochromator and detected by a cooled RCA C31034 photomultiplier tube. To obtain steady-state

spectral data, the incident light was chopped and the signal processed by a PAR lock-in amplifier. For processing pulsed signals a PAR boxcar averager triggered by the laser pulse was used. The time gate of the boxcar was either set to observe the fluorescence spectrum at a specific time after the laser pulse, or scanned to obtain the fluorescence as a function of time at a specific wavelength.

Figure 1 shows block diagrams of the experimental setups for time-resolved spectroscopy and PAS measurements.

III. GENERAL SPECTROSCOPY AND CONCENTRATION QUENCHING RESULTS

The absorption spectrum of $\text{NdP}_5\text{O}_{14}$ has been presented elsewhere.¹ It is similar to the spectrum of Nd^{3+} ions in other hosts with lower doping concentrations. The strongest absorption band occurs at approximately 8000 \AA , corresponding to the transition from the $^4I_{9/2}$ ground state to a band consisting of the unresolved components of the $^2H_{9/2}$ and $^4F_{5/2}$ levels (see the energy diagram of Nd^{3+} shown in Fig. 2). The second-strongest absorption band occurs near 5800 \AA , and is associated with the unresolved levels of the $^2G_{7/2}$ and $^4G_{5/2}$ levels. After absorption into any of the higher-energy levels, radiationless relaxation occurs to the $^4F_{3/2}$ metastable state. Fluorescence emission then takes place from the two crystal-field components of this level to the various Stark components of the 4I_J multiplets. Branching ratios determined previously⁷ indicate that most of the energy is emitted in the transitions terminating on the $^4I_{11/2}$ and $^4I_{9/2}$ levels centered around 1.06

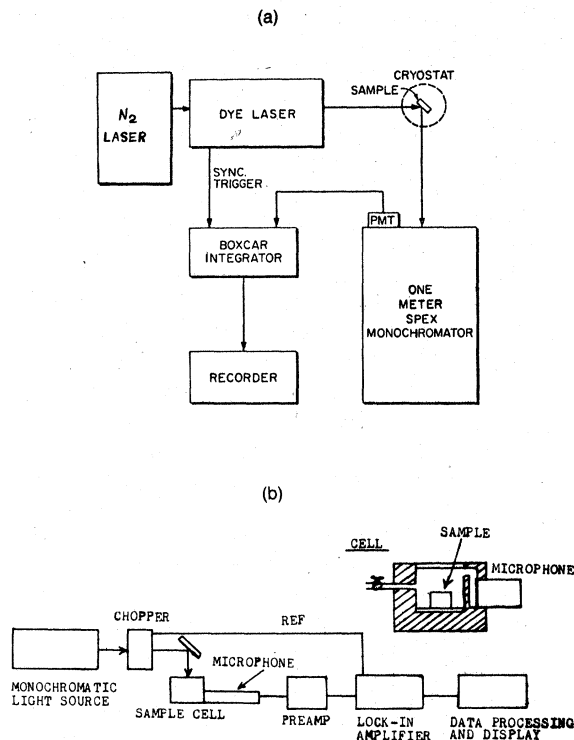


FIG. 1. (a) Block diagram of time-resolved spectroscopy setup. (b) Block diagram of photoacoustic spectroscopy setup.

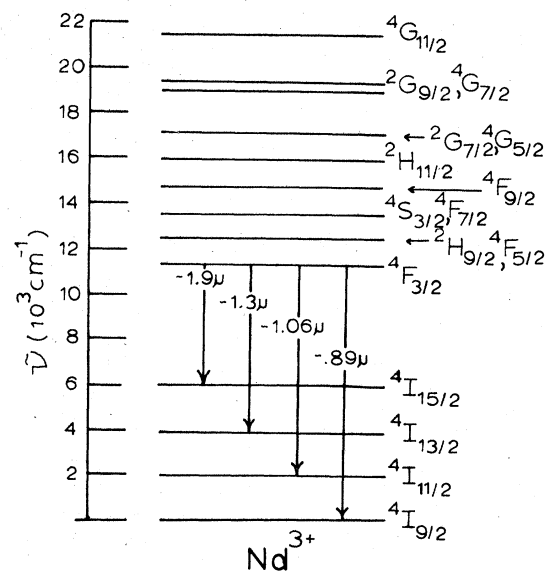


FIG. 2. Energy-level scheme of Nd^{3+} .

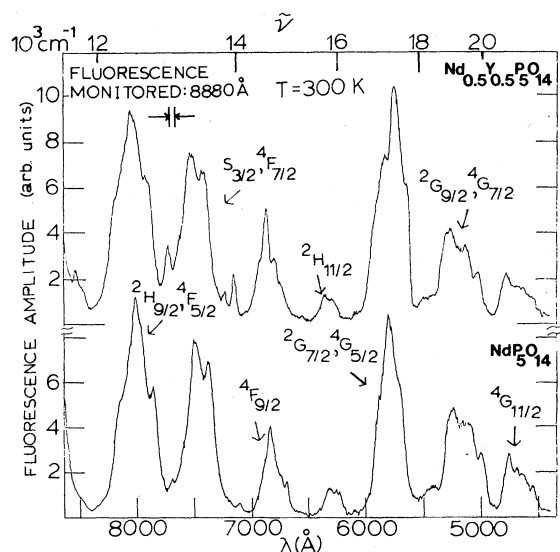


FIG. 3. Excitation spectrum of ${}^4F_{3/2}$ level in $\text{Nd}_{0.5}\text{Y}_{0.5}\text{P}_5\text{O}_{14}$ and $\text{NdP}_5\text{O}_{14}$ at 300 K.

μm and $0.89 \mu\text{m}$, respectively. The fluorescence spectrum is discussed in more detail in Sec. IV.

Figure 3 shows the fluorescence excitation spectra of the ${}^4F_{3/2}$ level monitored at 8880 \AA at room temperature for both $\text{NdP}_5\text{O}_{14}$ and a mixed crystal of $\text{Nd}_{0.5}\text{Y}_{0.5}\text{P}_5\text{O}_{14}$. The spectra are quite similar for the pure and mixed samples. In particular, the excitation bands centered at ~ 8000 and $\sim 5800 \text{ \AA}$ are comparable. The relative strength in the

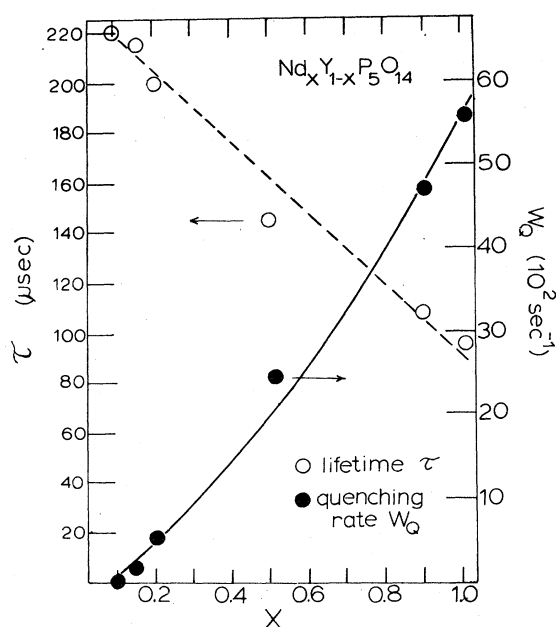


FIG. 4. Concentration dependence of the ${}^4F_{3/2}$ fluorescence lifetime and quenching rate for $\text{Nd}_x\text{Y}_{1-x}\text{P}_5\text{O}_{14}$ at 14 K. See text for explanation of the theoretical line.

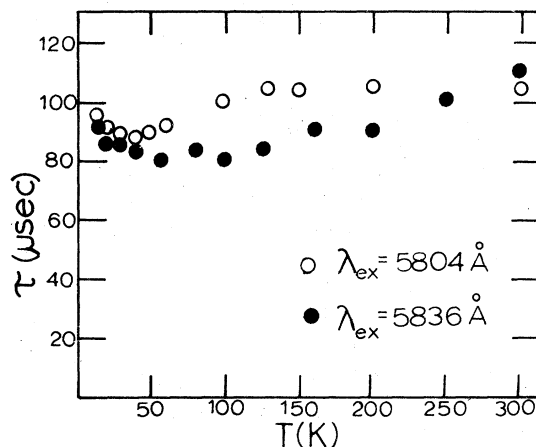


FIG. 5. Temperature dependence of the fluorescence lifetime of the ${}^4F_{3/2}$ level in $\text{NdP}_5\text{O}_{14}$ for laser-excitation wavelengths of 5804 \AA and 5836 \AA .

absorption spectrum of these two bands¹ correlated with the fact that the 8000-\AA excitation is approximately the same or less intense than the 5800-\AA band in the excitation spectrum suggests that the longer-wavelength band is less efficient in contributing to ${}^4F_{3/2}$ fluorescence than the shorter-wavelength band.

Figure 4 shows the fluorescence lifetime of the ${}^4F_{3/2}$ level at room temperature as a function of Nd concentration. The lifetime decreases from about $220 \mu\text{sec}$ for the $\text{Nd}_{0.1}\text{Y}_{0.9}\text{P}_5\text{O}_{14}$ sample to about $95 \mu\text{sec}$ for $\text{NdP}_5\text{O}_{14}$. A concentration-quenching rate can be defined

$$W_Q = \tau^{-1} - \tau_0^{-1}, \quad (1)$$

where τ_0 is the Nd fluorescence lifetime in the absence of any quenching interaction. This quenching rate is also plotted in Fig. 4 as a function of concentration. For an intrinsic lifetime of $\sim 220 \mu\text{sec}$, the plot of the quenching rate varies approximately as $x^{3/2}$.

The fluorescence lifetime of the ${}^4F_{3/2}$ level was measured with different wavelengths of excitation as a function of temperature between 14 and 300 K. The fact that a significant variation in lifetime with excitation wavelength was observed is discussed in Sec. IV. The temperature dependence of the fluorescence lifetime for $\text{NdP}_5\text{O}_{14}$ for two different wavelengths of excitation is shown in Fig. 5. There is a small increase in lifetime between 14 and 300 K. A similar trend is observed for other samples and other excitation wavelengths.

IV. TIME-RESOLVED SITE-SELECTION SPECTROSCOPY RESULTS

The optical spectral lines of impurity ions in solids all exhibit inhomogeneous broadening to some degree. This is due to the fact that imperfections and internal strains give rise to non-equivalent crystal-field sites for the impurity ions. In some cases the site differences are great enough so that transitions from ions in different types of sites can be distinctly resolved. High-resolution lasers have been used to selectively excite impurity ions in specific crystal-field sites in glass and crystal hosts. By tuning the laser excitation through an inhomogeneously broadened absorption band, it has been possible to observe significant variations in fluorescence spectral parameters such as peak positions, intensities, and radiative and radiationless transition probabilities.¹⁴ If pulsed lasers are used, time-resolved spectroscopy techniques allow the observation of the fluorescence spectrum at specific times after the laser pulse. After selective excitation of ions in specific sites, the fluorescence spectrum in some systems has been observed to evolve with time into spectra exhibited by ions in other types of sites. This implies that energy transfer is occurring between ions in different types of sites, and the observed time dependence can be used to characterize the properties of the energy transfer and help in identifying the mechanism responsible for the transfer process.

For investigating site-selection spectroscopy in the $\text{Nd}_x\text{Y}_{1-x}\text{P}_5\text{O}_{14}$ system, we pumped into the absorption band consisting of the unresolved $^2G_{7/2}$ and $^4G_{5/2}$ levels. The degree of site selection obtained with this pumping is somewhat surprising due to the number of overlapping levels and their homogeneous broadening resulting from radiationless relaxation processes. However, these transitions are known to be "hypersensitive" to changes in the local environment of the ion,^{11,15,16} and for other systems such as Nd in mixed garnet crystals we found that pumping into this level resulted in easily observable site-selection and energy transfer.¹⁷ The fluorescence was monitored from the $^4F_{3/2}$ level to the various components of the $^4I_{9/2}$ ground-state manifold in order to minimize homogeneous broadening of the transitions due to radiationless relaxation processes. As the narrow-line laser excitation was scanned across the broad absorption band at low temperature, for all of the samples investigated, changes in the relative fluorescence peak intensities, peak positions, and lifetimes were observed. For example, for the $\text{NdP}_5\text{O}_{14}$ sample at 14 K, the lifetimes ranged from 63 to 105 μsec , depending on the excitation

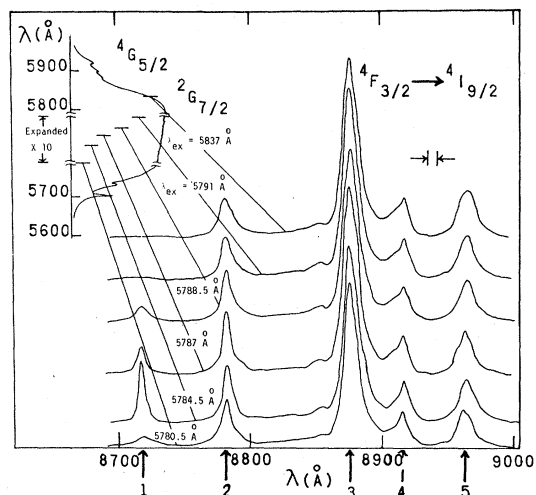


FIG. 6. $^4F_{3/2} \rightarrow ^4I_{9/2}$ fluorescence in $\text{NdP}_5\text{O}_{14}$ 20 μsec after selective excitation into different regions of the $^2G_{7/2}$, $^4G_{5/2}$ absorption band at 14 K.

wavelength, whereas at 300 K they varied between about 102 and 115 μsec . Figure 6 shows an example of the different fluorescence spectra that are obtained for the $\text{NdP}_5\text{O}_{14}$ sample at 14 K for pumping at different wavelengths. The distribution of the intensity among the five lines and the fluorescence lifetimes differ significantly. The lifetime is 67 μsec for 5785.5- \AA excitation and 77 μsec for 5837- \AA excitation. The highest-energy line (labeled 1 in Fig. 6) shows the greatest variation with pumping wavelength, but there are rela-

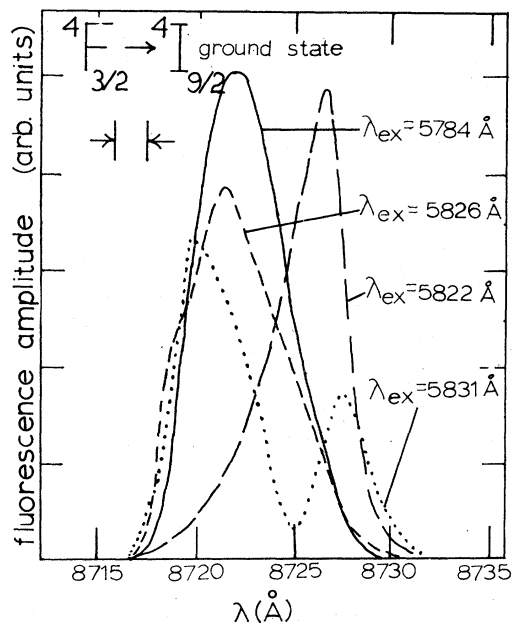


FIG. 7. Line 1 of $^4F_{3/2} \rightarrow ^4I_{9/2}$ fluorescence in $\text{Nd}_{0.5}\text{Y}_{0.5}\text{P}_5\text{O}_{14}$ after 20- μsec excitation at various wavelengths.

tive changes in the intensities of all of the other lines also. Figure 7 shows an expanded picture of line 1 as a function of excitation wavelength at 14 K for the $\text{Nd}_{0.5}\text{Y}_{0.5}\text{P}_5\text{O}_{14}$ crystal. Here the changes in line shape and peak position are quite evident. For the 5831-Å excitation the line is resolved into two distinct peaks.

The spectral as well as lifetime changes as a function of excitation wavelength can be attributed to the selective excitation of Nd ions in nonequivalent crystal-field sites. If rapid energy migration occurs among the Nd ions, the spectra should evolve with the time into some characteristic spectrum representing the average distribution of the energy among all of the ions in different types of sites. We attempted to observe this by monitoring the spectra as a function of time after the laser pulse in the range from 1 to 200 μsec . No significant time evolution of the spectra was detected in this range for either of the two samples investigated, $\text{NdP}_5\text{O}_{14}$ and $\text{Nd}_{0.5}\text{Y}_{0.5}\text{P}_5\text{O}_{14}$, for any wavelength of excitation at any temperature.

In order to quantitatively describe any time-dependent relative changes in the spectra obtained for two different excitation wavelengths, a fluorescence deviation function can be defined. The spectrum obtained for a given excitation wavelength is represented by a five-component function, each component corresponding to the ratio of the integrated intensity of one of the lines of the ${}^4F_{3/2} - {}^4I_{9/2}$ transitions to the total integrated intensity of all of the lines. Thus, each fluorescence spectrum can be characterized by a five-component vector. Any correlation between the fluorescence spectra for different excitation wavelengths can be seen by forming the vector difference between the functions describing the spectra for each excitation wavelength. Figure 8 shows typical results for the fluorescence deviation as a function of time after the laser pulse for both the $\text{NdP}_5\text{O}_{14}$ sample and the $\text{Nd}_{0.5}\text{Y}_{0.5}\text{P}_5\text{O}_{14}$ at various temperatures. A value of $D = 0$ would indicate an identical distribution of relative intensities in the five spectral lines for the two excitation wavelengths. The presence of energy transfer between Nd ions in different types of sites should result in a time-dependent decrease in D toward zero. Instead, for all cases investigated D remains, within experimental error, constant with time, indicating that no energy transfer is taking place between ions in nonequivalent sites.

The temperature dependence of the fluorescence deviation function for $\text{NdP}_5\text{O}_{14}$ is shown in Fig. 9. The error bars indicate the spread in the values of D for measurements at different times after the laser pulse at each temperature. Since the decrease in D with temperature occurs without

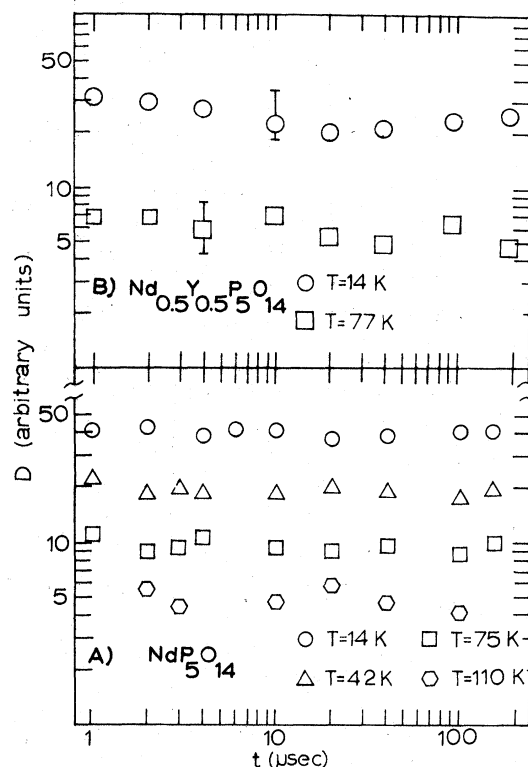


FIG. 8. (a) Time dependence of the fluorescence deviation function after excitation at 5784.5 and 5837 Å in $\text{NdP}_5\text{O}_{14}$ for temperatures of 14, 42, 75, and 110 K. (b) Time dependence of the fluorescence deviation function after excitation at 5805.5 and 5835 Å in $\text{Nd}_{0.5}\text{Y}_{0.5}\text{P}_5\text{O}_{14}$ for temperatures of 14 and 77 K.

any associated time dependence, this temperature dependence can be attributed to the reduced ability of the laser to selectively excite Nd ions in specific sites at high temperatures. This may be a result of homogeneous broadening of the absorption levels due to electron-phonon interactions.

The site-selection spectroscopy results pre-

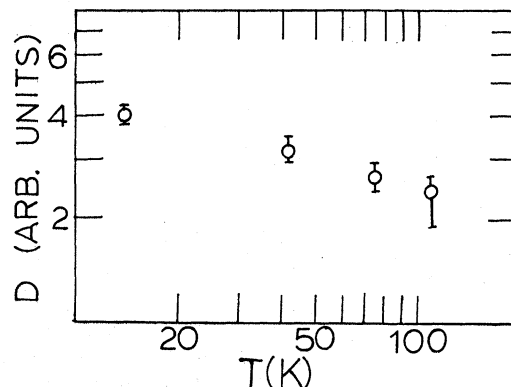


FIG. 9. Temperature dependence of the fluorescence deviation function after excitation at 5784.5 and 5837 Å in $\text{NdP}_5\text{O}_{14}$.

sented above show that Nd ions in pentaphosphate hosts occupy different types of crystal-field sites. Although the exact nature of these different sites is not known, they are probably due to differences in local strains resulting from structural imperfections and defects in the crystal. The fact that no energy transfer could be detected between ions in different types of sites is quite surprising in light of the fact that similar studies made on Nd ions in mixed garnet crystals show strong energy transfer between ions in nonequivalent sites.¹⁷ It is important to note, however, that spatial energy transfer between Nd ions in equivalent sites may take place without spectral energy transfer to ions in different types of sites. This type of transfer would not be observable by the time-resolved site-selection spectroscopy techniques used here, and is discussed further in Secs. VI and VII.

V. PHOTOACOUSTIC SPECTROSCOPY RESULTS

Photoacoustic spectroscopy techniques have recently been developed to characterize radiationless decay processes of ions in crystals.¹⁸⁻²¹ By comparing PAS results with fluorescence-excitation spectra, it has been possible to determine dominant relaxation channels.^{20,21} Low-resolution photoacoustic spectra were obtained at room temperature on the concentrated neodymium pentaphosphate samples. The 1000-W tungsten-halogen lamp chopped at 110 Hz was used as an excitation source. Figure 10 shows the results obtained on the $\text{NdP}_5\text{O}_{14}$ sample and the $\text{Nd}_{0.9}\text{Y}_{0.1}\text{P}_5\text{O}_{14}$. The signal-to-noise ratio on the more lightly doped samples was too poor to give meaningful results.

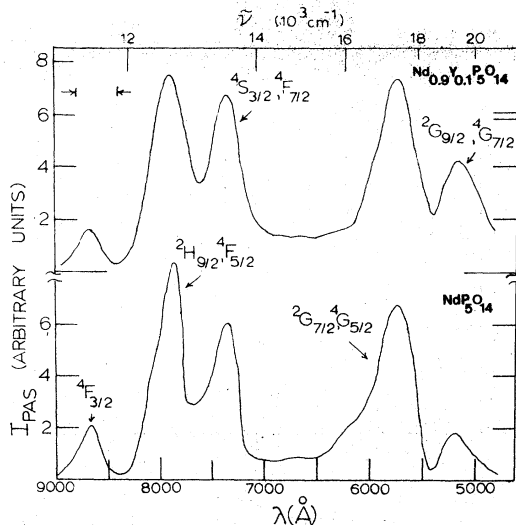


FIG. 10. Photoacoustic spectra of $\text{Nd}_{0.9}\text{Y}_{0.1}\text{P}_5\text{O}_{14}$ and $\text{NdP}_5\text{O}_{14}$ at 300 K.

Note that the relative peak heights of the major absorption bands in the PAS spectrum are comparable to those in the absorption and excitation spectra.

These PAS results are more difficult to interpret than those in the previous samples investigated.^{20,21} The photoacoustic signal normalized for the energy of the incident light beam at phase angle θ can be expressed as the sum over all the relaxation transitions that generate heat,²⁰

$$I_{\text{PAS}}(\theta) \propto N_a \sum_i \phi_m(i) h \nu_i \cos(\alpha_i - \theta) / N_0 h \nu_0, \quad (2)$$

where N_a is the number of photons absorbed, $\phi_m(i)$ is the fraction of excited atoms relaxing via the i th type of radiationless transition, $h \nu_i$ is the energy of the phonons emitted in the i th process, and α_i is the phase angle at which the signal due to transitions from the initial state of the i th transition is maximum. N_0 and $h \nu_0$ are the number and energy of the photons in the excitation beam. For the case of Nd^{3+} ions, the sum in Eq. (2) should include three different types of radiationless decay processes that occur during the relaxation of the ion from the level excited by the incident light. First, phonons will be emitted during the decay from the absorption state to the ${}^4F_{3/2}$ metastable level. Second, the ${}^4F_{3/2}$ level does not have unit radiative quantum efficiency, and, thus some amount of relaxation from this state to the ground state occurs radiationlessly. Third, the majority of the fluorescence transitions from the ${}^4F_{3/2}$ state terminate on levels of the 4I_J multiplets other than the ground state, and subsequent relaxation to the ground state occurs radiationlessly. Previous measurements have shown that there is virtually unit probability of relaxing to the metastable level after pumping into higher excited states.²² The radiative quantum efficiency of the ${}^4F_{3/2}$ level is of the order of ~ 0.9 in the absence of quenching interactions.²³ Most of the emission terminates on either the ${}^4I_{11/2}$ or the ${}^4I_{9/2}$ multiplets. Thus, from these considerations and the energy-level diagram shown in Fig. 2, it would seem that the higher-lying absorption bands should be more intense in the PAS spectrum compared to the lower-energy bands than in the absorption and excitation spectra due to the first type of decay processes listed above. This is the type of behavior observed in other samples.^{20,21} Figure 10 shows that this is not the case here, as exemplified by the fact that the 8000-Å band is equal or greater in intensity than the 5800-Å band.

This comparison of the absorption, excitation, and photoacoustic spectra indicates that there is relatively more radiationless quenching occurring

after excitation into the 8000-Å band than after excitation into the 5800-Å band. Since the absorption coefficients of these two bands are different, a different spatial distribution of excited ions will occur after excitation into each band. For such heavily concentrated systems as those considered here, the high absorption coefficient of the 8000-Å band will result in a significant fraction of the excited Nd ions being located close to the surface of the crystal. The somewhat smaller absorption coefficient for the 5800-Å band allows for more of the excited ions to be located farther into the bulk of the crystal. One mechanism to explain the spectral properties reported here is surface quenching, which is discussed in detail in Sec. VI.

VI. INTERPRETATION OF RESULTS

At this point it is worthwhile to summarize the experimental observations which must be explained by any viable model of concentration quenching in $\text{Nd}_x\text{Y}_{1-x}\text{P}_5\text{O}_{14}$ and similar materials. The quenching rate must vary less than quadratically with Nd concentration. Also it must have a very weak dependence on temperature, and it must be proportional to the absorption cross section. The quenching mechanism cannot lead to variations in oscillator strengths with Nd concentration, cannot result in spectral energy transfer, and cannot lead to nonexponential fluorescence decays. These requirements, along with quantitative theoretical predictions, place very rigid restrictions on developing an acceptable model for concentration quenching in these materials. The mechanism responsible for concentration quenching of Nd fluorescence in other types of materials such as $\text{Y}_3\text{Al}_5\text{O}_{12}:\text{Nd}^{3+}$ is cross relaxation between pairs of closely spaced ions. This leads to a quadratic dependence of the quenching rate on Nd concentration which is contrary to the linear dependence observed for the pentaphosphate hosts. The other common mechanism for concentration quenching which is observed in various materials is migration of the energy among the active ions until it reaches a sink where it is transferred to an ion that can dissipate the energy radiationlessly. This mechanism is not consistent with several of the requirements mentioned above. There is no dependence of the quenching rate on the absorption cross section in this model, and, generally, quenching by this mechanism has been found to lead to a strong temperature dependence. A quantitative estimate of the concentration of sinks necessary to give the observed quenching rate can be obtained in the fast-diffusion limit from the expression $W_Q = 4\pi DR_s C_s$, where D is the diffusion coefficient, R_s is the exciton trapping

radius at the sink, and C_s is the sink concentration. For the case of neodymium pentaphosphate a sink concentration of only 10 ppm of the Nd ions is necessary to cause the observed quenching rate, whereas site-selection spectroscopy shows that significant numbers of Nd ions exist in sites of different local perturbations without resulting in energy transfer or quenching.

Since the normal models for concentration quenching do not appear to apply to stoichiometric laser materials, it is necessary to develop a new model. One model that appears to meet all of the requirements outlined above is based primarily on surface quenching of the excitation energy. In this model the Nd ions on the surface of the sample act as sinks where the energy is dissipated radiationlessly. This gives a high concentration of sink sites but only in a very small region and not distributed uniformly throughout the sample. This situation will result in effective quenching for concentrated materials where the excitation energy is deposited near the sample surface, whereas it will be much less effective in lightly doped materials, where the energy is deposited more uniformly throughout the sample. Similarly for a given sample, quenching will be more effective where the absorption of exciting light is stronger due to the fact that more of the excited ions will reside closer to the surface. Weaker absorption bands will allow excitation energy to be deposited further into the crystal, resulting in less effective quenching.

To determine whether or not a surface-quenching model satisfies all of the necessary requirements for explaining the observed data, an expression for the quenching rate can be derived from simple geometric arguments based on the situation shown in Fig. 11. The incident light excites a Nd ion at a distance R from the surface of the crystal, and the energy can as an exciton migrate out from this site to other Nd ions. According to standard diffusion theory, after a time equal to the intrinsic lifetime of the exciton, the excitation energy will be found on one of the ions on the surface of a sphere of radius l , the diffusion length which is determined by

$$l = \sqrt{6D\tau_0}, \quad (3)$$

where τ_0 is the intrinsic lifetime of the exciton. If it is assumed that only excitons that migrate far enough to reach the surface are quenched, the quenching rate for an excited ion at depth R is

$$W_Q(R) = p\tau_0^{-1}(A'/A), \quad 0 \leq R \leq l \quad (4)$$

$$W_Q(R) = 0, \quad l < R,$$

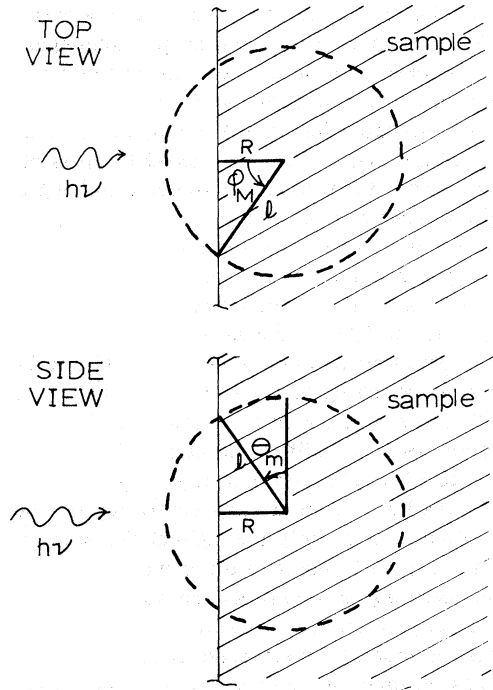


FIG. 11. Top and side-view geometry for excitation-energy migration in surface-quenching model.

where A is the area of the sphere of radius l , A' is the part of the area of this sphere that is outside the sample surface, and p is a factor to account for the probability of energy being dissipated radiationlessly instead of radiatively when it reaches the surface. The fraction of the area outside the sample can be found from the double integration

$$A = 2l \int_0^{\phi_M} d\phi \int_0^{\pi/2} \sin\theta d\theta \quad (5)$$

$$= 4l(l^2 - R^2)^{1/2} \cos^{-1}(R/l).$$

Thus the first part of Eq. (4) becomes

$$W_Q(R) = p(\tau_0\pi l)^{-1} \times (l^2 - R^2)^{1/2} \cos^{-1}(R/l), \quad 0 \leq R \leq l. \quad (6)$$

The observed fluorescence intensity is proportional to the concentration of excited ions. At time t the remaining concentration of excited ions which were originally created at a depth R into the sample is given by the product of the probability of exciting an ion at that position multiplied by the exponential decay function for such ions:

$$n_R^*(t) = \exp\{-t[\tau_0^{-1} + W_Q(R)]\} \times I_0\sigma C \exp(-\sigma CR) dR. \quad (7)$$

Here C is the concentration of Nd ions, σ is the

absorption cross section, and I_0 is the intensity of the incident light. The total concentration of excited Nd ions is found by integrating this expression over the entire thickness of the crystal T . Using Eqs. (4) and (6), this becomes

$$n^*(t) = \sigma C I_0 e^{-t/\tau_0} \left(\int_0^l \exp\{-tp(\tau_0\pi)^{-1}[1 - (R-l)^2]^{1/2} \times \cos^{-1}(R/l)\} dR + \int_l^T \exp(-\sigma CR) dR \right). \quad (8)$$

Evaluation of this expression shows that in this model the time dependence of the fluorescence intensity is described by

$$I(t) = I(0) \exp[-t(\tau_0^{-1} + 0.226p\sigma Cl\tau_0^{-1})]. \quad (9)$$

Thus, the quenching rate is given by

$$W_Q = 0.226p\sigma Cl\tau_0^{-1}. \quad (10)$$

The results of these considerations show that a surface-quenching model predicts exponential fluorescence decays and a quenching rate that varies linearly with the absorption cross section. Since the ion-ion interaction responsible for the migration is a resonant interaction, no thermal activation is necessary and only a weak temperature dependence is expected. The quenching rate should actually be somewhat greater at low temperatures, where there is less phonon scattering to limit the mean free path of the exciton. This appears to be verified by the lifetime data shown in Fig. 5. Quantitatively the experimentally observed quenching rate for neodymium pentaphosphate can be predicted by Eq. (10) if the thermal conversion probability for excitons reaching the surface (p) is taken to be unity and the diffusion length is of the order of 20 μsec . Previous estimates of the diffusion length of excitons in this material have ranged from 360 to 5000 \AA . A theoretical estimate for the diffusion coefficient can be obtained from the expression

$$D = |W_{\text{Nd-Nd}}|^2 R_{\text{nn}}^2 / \Delta\nu, \quad (11)$$

where ion-ion interaction rate, R_{nn} is the nearest-neighbor Nd separation, and $\Delta\nu$ is the exciton bandwidths. A rough estimate of the interaction rate can be found by assuming a nearest-neighbor electric dipole-dipole interaction for two ions in exact resonance,

$$W_{\text{Nd-Nd}} = \tau_0^{-1} (R_0/R_{\text{nn}})^6 (zC/C_T), \quad (12)$$

where z is the number of nearest-neighbor Nd sites, C_T is the Nd concentration in the unmixed sample, and the critical interaction distance R_0 is given by

$$R_0 = \left(\frac{3e^4 f^2 \Omega \tau_0}{8\pi^2 m^2 c^2 n^4 \bar{\nu}} \right)^{1/6} \quad (13)$$

Here f is the oscillator strength of the transition between the ground and metastable state, $\bar{\nu}$ is the average wave number in the region of spectral overlap, and Ω is the spectral overlap integral. For two overlapping Lorentzian lines,

$$\Omega = \frac{1}{\pi} \frac{\Delta\bar{\nu}_1 + \Delta\bar{\nu}_2}{(\Delta\bar{\nu}_1 + \Delta\bar{\nu}_2)^2 + (\bar{\nu}_1^0 + \bar{\nu}_2^0)^2}, \quad (14)$$

where $\bar{\nu}^0$ is the peak position and $\Delta\bar{\nu}$ is the Lorentzian contribution to the linewidth. Thus for perfect overlap Ω is proportional to the inverse of the homogeneous contribution to the spectral linewidth. In most cases this is not possible to measure by normal spectroscopy methods when the transition terminates on the ground state and no significant contributions are present from relaxation processes. Saturation and coherent transient spectroscopy investigations have found homogeneous linewidths of transitions of this type to be of the order of 10^7 Hz.²⁴ This can be used in Eq. (13), which leads to a predicted value of 51 Å for R_0 . Then for transitions out to fifth-nearest neighbors, a distance of 7.4 Å, Eq. (12) predicts an ion-ion interaction rate of 9.1×10^9 sec⁻¹. Substituting these numbers into Eq. (11) yields a predicted diffusion coefficient of 3×10^{-2} cm² sec⁻¹. Then substituting this result into Eq. (3) gives a predicted diffusion length of about 63 μm, which is consistent with the value needed to interpret the concentration-quenching data with a surface-quenching model.

Although each Nd ion has only one true nearest-neighbor site in the NdP₅O₁₄ lattice structure, there are eight Nd sites within an 8 Å radius. Thus for the high concentrations used here, every Nd ion will always have other Nd ions close by for efficient energy transfer. The use of Eqs. (3), (11), and (12) in Eq. (10) shows that the quenching rate should vary as $C^{1.5}$. This is consistent with experimental data as shown by the solid line in Fig. 4.

An attempt was also made to fit the data with a surface-quenching model in which the excitation energy did not diffuse, but rather was transferred to the surface ions in a single-step electric dipole-dipole process. The predictions of this model were not consistent with the observed results, because they predicted a nonexponential decay time and quantitatively an unphysically large value for the interaction strength had to be assumed to give the correct magnitude for the quenching rate.

A direct check was made on the prediction that the quenching rate is proportional to the absorption

cross section by monitoring the fluorescence lifetime as the laser excitation was scanned from the peak to the wings of the absorption band. The results obtained at 14 K for the NdP₅O₁₄ sample are shown in Fig. 12. There is an obvious increase in fluorescence lifetime, and thus a decrease in the quenching rate as the excitation is scanned from the region of high absorption to one of small absorption as predicted. However, the dependence of W_0 on σ appears to be less than the linear dependence predicted by Eq. (10). There may be several reasons for this. First, it is difficult to change the laser wavelength without also altering its power and beam position. Thus, it is impossible to exactly repeat the experimental conditions from point to point in Fig. 12, and only the general trend of the data can be considered important. Also the theoretical derivation of Eq. (10) is based on the assumption that the number of photons absorbed from the incident beam at depth R is directly proportional to the absorption cross section. This is only true for small values of the absorption coefficient. The exact expression is

$$n = n_0 [1 - \exp(-\sigma CR)] \\ = n_0 \sigma CR \left[1 - \frac{1}{2} \sigma CR + \frac{1}{6} (\sigma CR)^2 - \dots \right], \quad (15)$$

and, thus for the high optical densities treated here the variation with the absorption cross section should be less than linear. The linear approximation was made in deriving Eq. (10) only to simplify the calculations.

In order to determine whether the lifetime change shown in Fig. 12 is due to the change in absorption strength and not a result of selectively exciting ions in different sites having different energy-

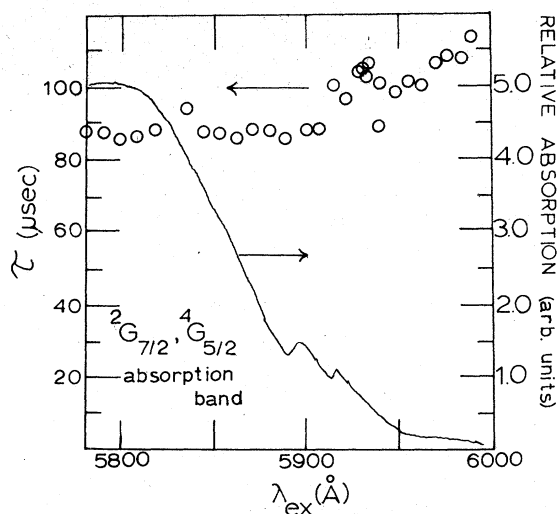


FIG. 12. $4F_{3/2}$ fluorescence lifetime vs wavelength of laser excitation at 14 K along with laser-probed absorption band at 300 K for NdP₅O₁₄.

transfer characteristics, we measured the decay time after pumping into the ${}^4G_{11/2}$ band near 4700 Å. The peak absorption strength of this band is significantly less than that of the 5800-Å band, and the lifetime is measured to be significantly greater, around 110 μsec at 14 K. It was difficult to scan the excitation into the wings of this band and measure the lifetime change because of the much weaker fluorescence signal. However, the trend again appeared to be toward longer lifetimes on the band edge. No shorter lifetimes were detected. Thus, we conclude that the lifetime change in Fig. 12 is associated with the change in absorption strength and not just site selectivity.

There is still a question as to the exact mechanism for quenching after the exciton has migrated to the surface. The energy levels of the surface ions may be perturbed in such a way that they act as sinks or allow for cross-relaxation to occur with other Nd ions. A third possibility is that there is such a high density of excited Nd ions on the surface that biexcitonic processes are responsible for the quenching. The latter possibility was investigated by monitoring the fluorescence lifetime as a function of laser power for the $\text{NdP}_5\text{O}_{14}$ sample at 14 K. The excitation was near the peak of the 5800-Å band, and the power was decreased by a set of calibrated neutral density filters. The fluorescence lifetime was found to increase slightly with decreased laser intensity. This suggests that some amount of exciton-exciton interaction may be taking place. However, the dependence of W_Q on laser power does not appear to be strong enough to account for all of the quenching, and most probably several different mechanisms are taking place at the same time.

VII. DISCUSSION AND CONCLUSIONS

The surface-quenching model described in Sec. VI is consistent with all of the results obtained in this investigation. It also appears to be consistent with data reported by other workers. Similar surface-quenching effects have also been observed in other types of materials with high absorption coefficients such as aromatic hydrocarbon crystals.²⁵

For crystals with high absorption coefficients, radiative reabsorption effects should be expected. We attempted to determine the extent of such effects by observing the fluorescence lifetime as a function of sample alignment. The lifetime appeared to lengthen slightly in going from front-face to back-face illumination. The former configuration was used to minimize radiative reabsorption effects.

It should be pointed out that there is a possible alternative explanation for the fact that the relaxa-

tion processes in the excited states do not appear to contribute to the PAS signal. This would be true if the decay occurred radiatively instead of radiationlessly. There has been some weak fluorescence observed between 1.4 and 1.7 μm which has not been explained.⁷ However, this was observed, only at a high level of excitation and only at room temperature and, thus cannot generally account for all of the observed quenching characteristics.

It is still not clear exactly why the fluorescence quenching rate is so much less in $\text{NdP}_5\text{O}_{14}$ than in YAlG:Nd . One obvious difference is that there is less resonance between the ${}^4F_{3/2} \rightarrow {}^4I_{15/2}$ emission transitions and the ${}^4I_{9/2} \rightarrow {}^4I_{15/2}$ absorption. Also a distinguishing feature of the pentaphosphate host is that the Nd ions are fairly isolated from each other and do not share the same oxygen ion.⁴ Another interesting observation is that the quenching of Nd fluorescence in phosphate glass hosts is also significantly less than for other glasses.²⁶ Which of these features is most important in determining the quenching characteristics is not evident. It is known that hydrogen and other impurity ions are very effective in quenching the fluorescence in these materials.²⁷ These impurities may perturb the energy levels of neighboring Nd ions to allow stronger quenching interactions to occur. The energy levels of surface ions may similarly be perturbed.

The diffusion coefficient of the order of $\sim 10^{-2}$ $\text{cm}^2 \text{sec}^{-1}$ determined for $\text{NdP}_5\text{O}_{14}$ is significantly greater than the typical values of D that range between 10^{-9} to 10^{-14} $\text{cm}^2 \text{sec}^{-1}$ for energy migration among other systems of rare-earth ions in solids.²⁸ The reason for this is primarily the higher concentration of Nd ions. In other highly concentrated systems, exciton diffusion coefficients of this magnitude have been found.^{25,29,30} This results in efficient spatial diffusion without spectral diffusion. As the excitation energy migrates near to a spectrally different site, there are always a significant number of ions nearby in equivalent sites that favor transfer. Only at the surface is there a significant concentration of perturbed ions to cause effective quenching. The fact that the exciton diffusion length is greater than the effective thermal diffusion length¹⁹ minimizes the contribution of excited-state relaxation phonons to the photoacoustic signal, and enhances the contribution of the radiationless quenching at the surface.

In summary, the results of time-resolved site-selection spectroscopy, PAS, and other investigations presented here are consistent with a model involving spatial energy migration without spectral diffusion which results in significant radiationless quenching at the surface.

ACKNOWLEDGMENTS

The authors gratefully acknowledge discussions with L. A. Riseberg, the information supplied by M. J. Weber concerning quenching in phosphate

glass hosts, discussions with M. G. Rockley on PAS, and thank J. G. Gualtieri for suggesting this problem and supplying us with the samples. This work was supported by the U. S. Army Research Office.

- *Present address: GTE-Sylvania Laboratories, Danvers, Mass.
- ¹S. R. Chinn, H. Y.-P. Hong, and J. W. Pierce, *Laser Focus* **12**, 64 (1976).
- ²H. G. Danielmeyer and H. P. Weber, *IEEE J. Quantum Electron* **8**, 805 (1972).
- ³H. G. Danielmeyer, *Festkörperprobleme* **15**, 253 (1975).
- ⁴H. P. Weber, *Opt. Quantum Electron* **7**, 431 (1975).
- ⁵S. Singh, D. C. Miller, J. R. Potopowicz, and L. K. Shick, *J. Appl. Phys.* **46**, 1191 (1975).
- ⁶W. Strek, C. Szafranski, E. Lukowiak, Z. Mazurak, and B. Jezowski Trzebiatowska, *Phys. Status Solidi A* **41**, 547 (1977).
- ⁷M. Blätte, H. G. Danielmeyer, and R. Ulrich, *Appl. Phys.* **1**, 275 (1973).
- ⁸B. C. Tofield, H. P. Weber, T. C. Damen, and P. F. Liao, *J. Solid State Chem.* **12**, 207 (1975).
- ⁹A. Lempicki, *Opt. Commun.* **23**, 376 (1977).
- ¹⁰H. G. Danielmeyer, *J. Lumin.* **12/13**, 179 (1976).
- ¹¹F. Auzel, *IEEE J. Quantum Electron.* **12**, 258 (1976).
- ¹²P. P. Liao, H. P. Weber, and B. C. Tofield, *Solid State Commun.* **16**, 881 (1973).
- ¹³J. M. Flaherty and R. C. Powell, *Solid State Commun.* **26**, 503 (1978).
- ¹⁴C. Brecher, L. A. Riseberg, and M. J. Weber, *Appl. Phys. Lett.* **30**, 475 (1977); C. Brecher and L. A. Riseberg, *Phys. Rev. B* **13**, 81 (1976); M. D. Kurz and J. C. Wright, *J. Lumin.* **15**, 169 (1977); R. K. Watts and W. C. Holton, *J. Appl. Phys.* **45**, 873 (1974); C. Hsu and R. C. Powell, *Phys. Rev. Lett.* **35**, 734 (1975); C. Hsu and R. C. Powell, *J. Phys. C* **9**, 2467 (1976); G. E. Venikouas and R. C. Powell, *Phys. Rev. B* **17**, 3456 (1978); R. Flach, D. S. Hamilton, P. S. Selzer, and W. M. Yen, *ibid.* **15**, 2348 (1977); P. M. Selzer, D. S. Hamilton, and W. M. Yen, *Phys. Rev. Lett.* **38**, 858 (1977); J. Koo, L. R. Walker and S. Geschwind, *ibid.* **35**, 1669 (1975); N. Motegi and S. Shionoya, *J. Lumin.* **8**, 1 (1973); and L. A. Riseberg and W. C. Holton, *Opt. Commun.* **9**, 298 (1973).
- ¹⁵F. Auzel, *Ann. Telecommun.* **24**, 199 (1969).
- ¹⁶B. R. Judd, *Phys. Rev.* **127**, 750 (1962).
- ¹⁷M. Zokai and R. C. Powell, *Bull. Am. Phys. Soc.* **23**, 202 (1978).
- ¹⁸A. Rosencwaig, *Opt. Commun.* **7**, 305 (1973); *Anal. Chem.* **47**, 593 (1975).
- ¹⁹J. C. Murphy and L. C. Aamodt, *J. Appl. Phys.* **48**, 3502 (1977); L. C. Aamodt, J. C. Murphy, and J. G. Parker, *ibid.* **48**, 927 (1977).
- ²⁰L. D. Merkle and R. C. Powell, *Chem. Phys. Lett.* **46**, 303 (1977).
- ²¹R. G. Peterson and R. C. Powell, *Chem. Phys. Lett.* **53**, 366 (1978).
- ²²H. P. Weber and B. C. Tofield, *IEEE J. Quantum Electron.* **11**, 368 (1975).
- ²³H. P. Weber, P. F. Liao, and B. C. Tofield, *IEEE J. Quantum Electron.* **10**, 563 (1974).
- ²⁴A. Z. Genack, R. M. Macfarlane, and R. G. Brewer, *Phys. Rev. Lett.* **37**, 1078 (1976); A. Szabo, *ibid.* **25**, 924 (1970); L. E. Erickson, *Phys. Rev. B* **16**, 4731 (1977).
- ²⁵R. C. Powell and Z. G. Soos, *J. Lumin.* **11**, 1 (1975).
- ²⁶M. J. Weber (private communication).
- ²⁷B. C. Tofield, H. P. Weber, T. C. Damen, and G. A. Pasteur, *Mat. Res. Bull.* **9**, 435 (1974).
- ²⁸R. K. Watts, in *Optical Properties of Ions in Solids*, edited by B. DiBartolo (Plenum, New York, 1975).
- ²⁹F. J. Himpfel, V. Saile, N. Schwentner, M. Skibowski, E. E. Koch, and J. Jortner, *J. Chem. Phys.* **65**, 5226 (1976).
- ³⁰C. E. Bleil and I. Broser, *J. Phys. Chem. Solids* **25**, 11 (1964).